Switch-Driving Eddy-Current Displacement Sensing Based on Power Loss

Zhong Jianpeng[1,a], Li Lichuan[1,b]
[1]School of Electrical Engineering, Xi'an Jiaotong University, Xi'an, 710049, China
[a]jp.zhong333@stu.xjtu.edu.cn, [b]lcli@mail.xjtu.edu.cn

Abstract: The principle of a switch-driving eddy-current displacement sensor is analyzed based on the eddy current power loss. This sensor converts the power loss into a working current by using switching circuits, in which a DC current related to the gap is picked out with a low pass filter. The displacement of the target thus could be obtained. A series of static experiments are carried out with iron, aluminum and nonmagnetic stainless steel as the targets, finally giving promising results.

Keywords: Eddy-Current Sensor, Switching Circuits, Power Loss, Resonance Frequency

Introduction

Magnetic bearings are presently being viewed as a good substitute for the rolling bearings utilized in the rotating machinery due to its attractive advantages of contactless, low friction, no lubrication and long working life, etc [1]. However, in order to guarantee its stable levitation, it's necessary to get the accurate position information of the rotor by a displacement sensor. J. Boehm *et al.* [2] discussed various characteristics of sensors available in magnetic bearings, and pointed out that the most versatile sensor type for magnetic bearings is the eddy current sensor (ECS).

Preliminary investigations as to the ECS revealed that diverse methods are adopted for the displacement sensing. Tan *et al.* [3] discussed the basic working principle of the ECS, and introduced three concrete types of sensors based on the resonance testing. In [4], the authors indicated drawbacks of the traditional LC parallel resonance testing ECS, and proposed a new type of ECS based on a resonant impedance inversion method. Differing from the resonance sensing, Girgis *et al.* [5] designed two types of sensors to measure mechanical vibrations by means of demodulating the output voltage. In [6], a fully integrated inductive proximity ECS based on the principle of a differential relaxation oscillator had been realized.

Although the testing principles of the above-mentioned sensors are different from each other, a high frequency sinusoidal current source usually is used and a series of complicated conditioning circuits are needed in these sensors. Instead of the sinusoidal exciter, L. Li [7] proposed a new switch-driving ECS based on the power loss; moreover, this design could simplify the conditioning circuits. Briefly, the principle of this ECS is similar to that of an electromagnetic oven (see Fig. 1). The current flowing in the wire is closely related to the distance between the pan and the oven. The closer the pan is from the oven, the greater the current becomes.

In this paper, we make a further analysis on the principle of the ECS proposed in [7], and an experiment setup is established to verify the theoretical analysis. Iron, aluminum and nonmagnetic stainless steel are chosen as the targets. A series of static experiments are carried out, and the dependence of the system sensitivity on different parameters is presented.

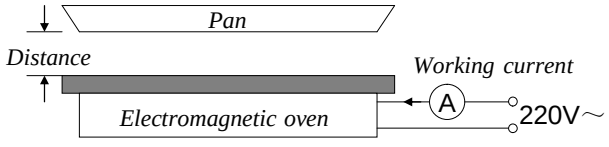

Fig. 1. Diagram of the electromagnetic oven

Principles and Circuits Analysis

In this section, we summarize the working principle of this ECS. As can be seen in Fig. 2, R and L are the coil copper resistance and the coil inductance respectively, C is a series capacitor connecting with the sensing coil, K_1 and K_2 are two perfect switches, and two MOSFETs are used here in practical applications, R_s is a conversion resistor for converting the working current into a voltage signal as the primary output, and U is a DC voltage source for the ECS system.

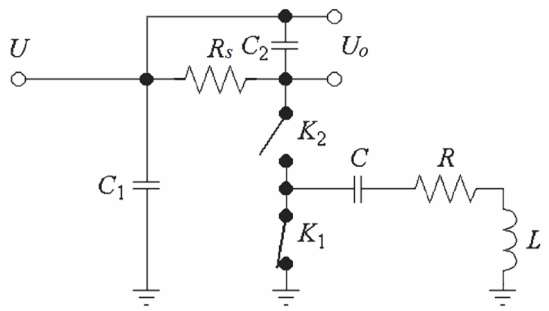

Fig. 2. Circuit for power-loss-based current sensing

Under the on-and-off control of perfect switching circuits, the DC voltage U is converted into an ideal periodic square-wave signal for supplying the testing circuits (consisting of the sensing coil and the series capacitor C), if the resistor R_s is non-existent ($R_s = 0$). As to the RLC series second–order linear system with the square-wave exciter, it seems difficult to analyze the circuits by solving the differential equation due to the variation of parameters. From the point of the view of the power loss, however, the essence of the system with different parameters is the same.

As the switch K_2 turns on (corresponding with the positive period of square-wave signal), the electrical current flows through R_s, K_2, C, the sensing coil and the ground in sequence. Considering different parameters, there may be a power feedback process before the supply of power (see Fig. 3) due to the continuity of electrical current. Where $t \in (t_1, t_2)$, $i(t) < 0$, the power fed by the circuits is

$$W_f = \int_{t_1}^{t_2} Ui(t)dt < 0 . \tag{1}$$

While $t \in (t_2, t_3)$, $i(t) > 0$, the power supplied by the source is presented as follows,

$$W_p = \int_{t_2}^{t_3} Ui(t)dt > 0 . \tag{2}$$

On the contrary, as the switch K_1 turns on, the coil current flows through a closed path formed from K_1, C and the sensing coil. However there is no current flowing through R_s at this stage.

Obviously, only the resistive elements dissipate the electrical energy, and the power loss, at two different stages of switching circuits, is entirely supplied by the voltage source as the K_2 is on. The working current $i(t)$ flowing through the resistor R_s is a periodic signal containing a positive DC component i_{dc}.

Consequently, within a whole switching period T, $t \in (t_0, t_3)$, the power is calculated as

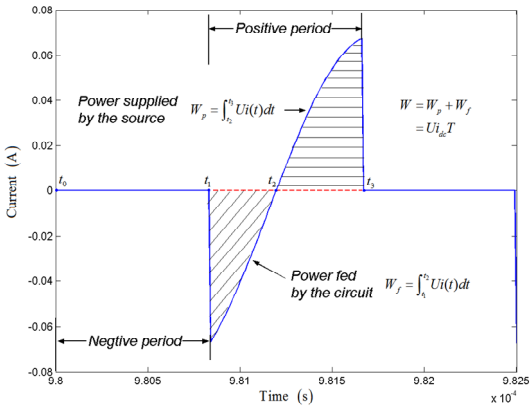

Fig. 3. Typical working current waveform

$$W = W_p + W_f = \int_{t_0}^{t_3} Ui(t)dt = Ui_{dc}T \ . \tag{3}$$

According to the weakly coupled transformer model of the ECS [8], the equivalent impedance Z is a one-variable function about the gap x for a designed ECS and a determinate target. Moreover, the change in the impedance is actually induced by the variation of the power loss, as the gap varies. Therefore, although it is difficult to get the analytical derivation, there must be a definitive functional relation between the gap x and the DC component i_{dc}. By sensing the DC current component, we could get the displacement information of the target, which could be achieved simply with a low pass filter consisting of R_s and C_2 (see Fig. 2).

Measurement Results

In this section, we firstly introduce the experiment setup established for the feasibility test of the ECS, and then discuss the variation of the sensitivity on different parameters (including DC voltage U, switching frequency f and conversion resistor R_s).

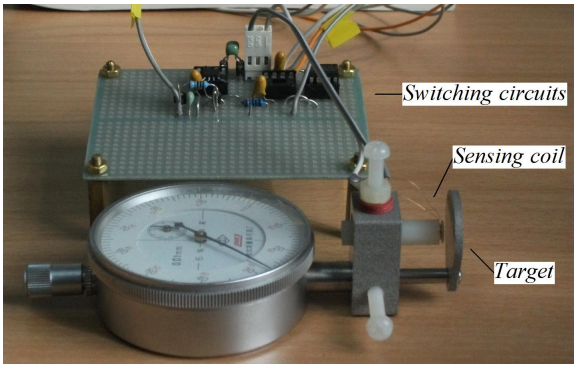

Fig. 4. Experimental facility

Experimental facility. As illustrated in Fig. 4, the experimental facility is set up. The switching circuits are constructed of MOSFETs, and the control signal is produced by a signal nerator. The sensing coil has 36 turns with an air core inductance L of $6.2\mu H$ and a copper resistance R of 1.9Ω. The targets consist of iron, aluminum and nonmagnetic stainless steel. The distance between the target and the coil is measured by a dial indicator.

According to the formula of the resonance frequency of RLC series circuits, the testing circuits would be in critical damping if a series capacitor of $6.87\mu F$ is selected. In our actual circuits, a capacitor of $0.02\mu F$ is connected to the sensing coil in series, thus, the system is in under damping in effect, and the resonance frequency is about $452kHz$.

Variation of sensitivity on f. We regard the above resonance frequency as a reference and then select $100kHz$, $200kHz$, $300kHz$, $400kHz$, $500kHz$, $750kHz$, $1MHz$ and $1.5MHz$ as the switching frequencies. The DC voltage U of $5V$ and the conversion resistor R_s of 1Ω are the other two invariable parameters. In this case, a series of static experiments are carried out and results are obtained.

From the original data derived, we find that the variation tendencies of the sensitivity on different switching frequencies are not identical, that is, the DC current component i_{dc} is not always increased or reduced along with the increase of the gap x. For example, as the switching frequencies are $400kHz$ and $500kHz$ respectively, and the measured target is iron, the curve of i_{dc} vs. x is depicted in Fig. 5.

In both cases, any DC current has a satisfactory relative variation over the gap span of 1mm, and the linearity of the sensor is maintained well over the span of 0-0.5mm. However, as the range is extended to 1mm, both the linearity and the sensitivity deteriorate quickly.

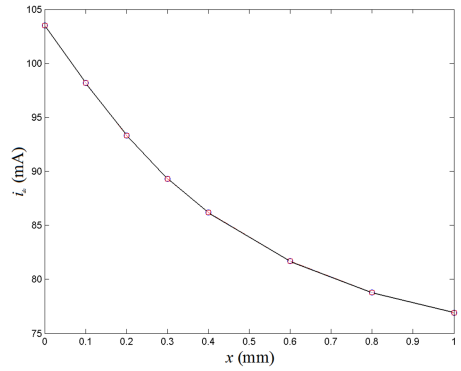

(a) 400kHz

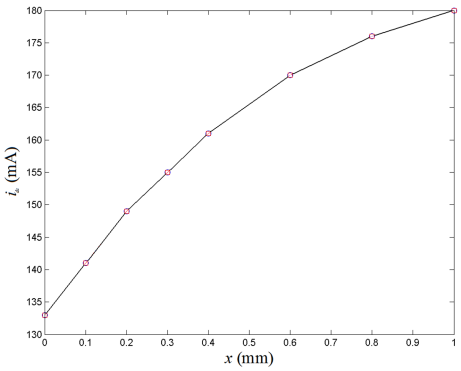

(b) 500kHz

Fig. 5. Dependence of i_{dc} on gap x with single coil

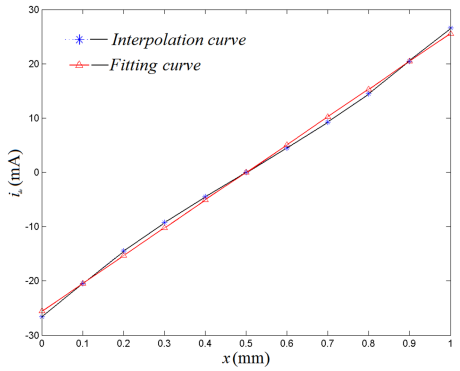

(a) 400kHz

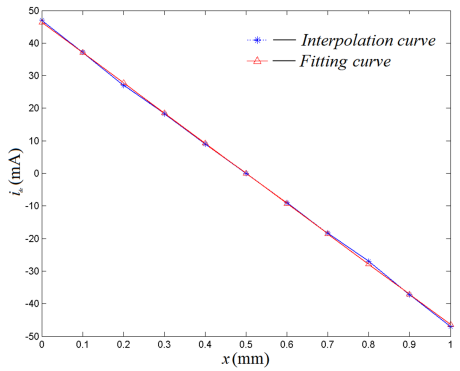

(b) 500kHz

Fig. 6. Dependence of i_{dc} on gap x with dual coil

In order to extend the linear range, we suppose that another identical coil is existing by the opposite side of the target with the basic gap of 0.5mm, and the data acquired with two coils are the same, thus, we could get an output line by dealing with the original data with the linear least squares fitting method. The slope of the line is the sensitivity.

The linear range of the sensor expands after the differential measurement treatment (see Fig. 6). The linearity is maintained within 2% over the span of 1mm and the sensitivity is 2 times the original gained with a single coil. Undergoing this treatment, we could get the curves of the sensitivity and the linearity about different switching frequencies against different measured targets, which are presented in Fig. 7.

From Fig. 7, several conclusions could be reached as follows:

1) With the increase of the switching frequency, the sensitivity against different targets experiences an approximately identical variation process. The sensitivity reaches a negative maximal value as the switching frequency is chosen within a narrow range of the both sides of the resonance frequency, however, while the switching frequency is more and more far from the resonance frequency, the sensitivity changes from negative to positive and becomes more and more low.

2) Although the switching frequency is far from the resonance frequency, the sensitivity is still considerable and has two positive maximal values. As to iron, the left maximal value is even bigger, but to the nonmagnetic materials (aluminum and nonmagnetic stainless steel), it is the other way around. As two different switching frequencies are selected at about half and 1.5 times the resonance frequency (corresponding with the two positive maximal values), the primary-measuring average sensitivity with different targets is 5.4mA/mm (iron), 17.1 mA/mm (aluminum) and 12.8mA/mm (nonmagnetic stainless steel) respectively, and the li-

nearity is usually maintained within 2%.

3) The sensitivity against the ferromagnetic material is obviously higher than that against the nonmagnetic materials as the switching frequency is in the nearby range of the resonance frequency. To the nonmagnetic materials, the sensitivity against aluminum is higher than that against nonmagnetic stainless steel due to the difference of the electrical conductivity.

Variation of sensitivity on U. In this section, the influence of different DC voltages ($U=1\text{V}$ or $U=5\text{V}$) on the performance of the sensor is discussed. The other parameters, such as switching frequency and the conversion resistor, all keep invariable as they are in previous section. Treating the original data in differential measurement mode like before, only the variation of the sensitivity against iron is shown in Fig. 8 owing to the similarity of the variation of sensitivity against different targets.

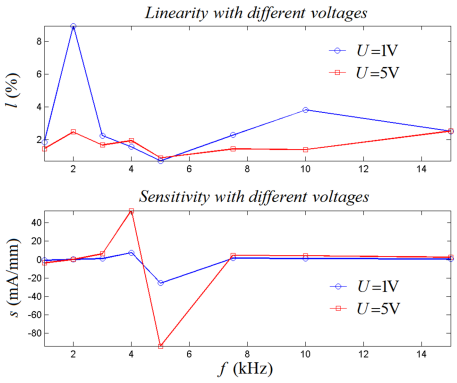

Fig. 8. Variation of sensitivity on voltage (iron)

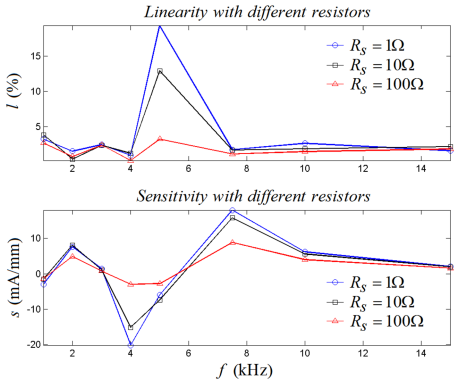

Fig. 9. Variation of sensitivity on resistor (nonmagnetic stainless steel)

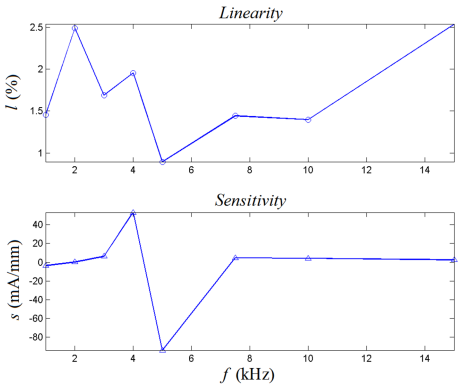

(a) Iron

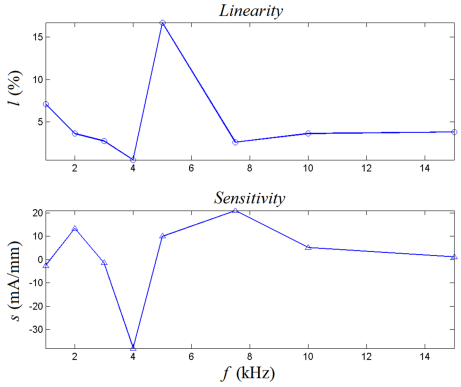

(b) Aluminum

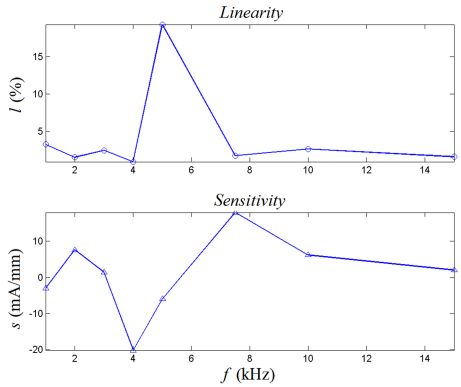

(c) Nonmagnetic stainless steel

Fig. 7. Variation of sensitivity on frequency

Having nothing with the characteristic of targets, the sensitivity generally has a considerable improvement as the DC voltage varies from 1V to 5V, especially in the nearby range of the resonance frequency, the increase margin is the largest. Meantime, the linearity of the sensor has an improvement in some frequency range.

Variation of sensitivity on R_s. To analyze the influence of the conversion resistor R_s on the sensor, three resistors of 1Ω, 10Ω and

100Ω are individually utilized in the circuit. The DC voltage is 5V and the switching frequencies still keep invariable like before.

As shown in Fig. 9, a larger conversion resistor will cause a smaller current, thus the sensitivity is reduced, whereas the linearity is improved.

Conclusions

The principle of a switch-driving eddy current displacement sensor is analyzed and a series of static experiments are carried out to verify the theoretical analysis. Based on the analysis of the data obtained, we could get several conclusions as follows:

1) For a sensor of the testing circuits including the series capacitor, the sensitivity would be the greatest as the switching frequency is restricted to the resonance frequency. Besides, the switching frequency also could be selected at the frequency of approximately half or 1.5 times the resonance frequency.

2) A high DC voltage will improve the sensitivity, whereas it also leads to the problem of temperature rise. Therefore it is proper to choose a DC voltage that could produce a small absolute current value (e.g. less than 30mA) and has a large relative variation of the current (e.g. more than 30% of the minimum DC current) over the gap span.

3) A conversion resistor is necessary to get the voltage output. Considering the influence of the resistor on the sensitivity, the smaller the resistor is, the better the performance is.

References

[1] B. Shafai, S. Beale, P. LaRocca, and E. Cusson. Adaptive forced balancing for multivariable systems, ASME Journal of Dynamic Systems, Measurement, and Control, Vol. 117, 496-502, 1995.

[2] J. Boehm, R. Gerber, N.R.C. Kiley. Sensors for magnetic bearings, IEEE Trans. Magn. Vol.29, No. 6, 2962-2964, 1993.

[3] Tan Zu-Gen, Cheng Shou-Chuan. The analysis and parameter selection on the fundamental of eddy current transducers, Chinese Journal of Scientific Instrument. Vol. 1, No. 1, 113-122, 1980.

[4] D. Vyroubal, D. Zele. Experimental optimization of the probe for eddy-current displacement transducer, IEEE Trans. Instrum. Meas. Vol. 42, No. 6, 995-1000, 1993.

[5] G. A. Girgis, K. Horn, G. Kruse. Measurement of mechanical vibrations using eddy current transducers and simple digital demodulating techniques, IEEE Trans. Ind. Electron. Vol. 35, No. 1, 135-140, 1988.

[6] Ph. A. Passeraub, P. – A. Besse and A. Bayadroun et al. First integrated inductive proximity sensor with on-chip CMOS readout circuit and electro deposited 1mm flat coil, Sensors and Actuators A 76 (1999) 273-278.

[7] Lichuan Li. Eddy-current displacement sensing using switching drive where baseband sensor output is readily available, IEEE Trans. Instrum. Meas. Vol. 57, No. 11, 2548-2553, 2008.

[8] G. Y. Tian, Z. X. Zhao, R. W. Baines. The research of inhomogeneity in eddy current sensors, Sensors and Actuators A69 (1998) 148-151.